



Published in final edited form as:

Nat Med. 2014 September ; 20(9): 1018–1026. doi:10.1038/nm.3587.

A mammalian acetate switch regulates stress erythropoiesis

Min Xu¹, Jason S. Nagati¹, Jian Xie¹, Jiwen Li¹, Holly Walters², Young-Ah Moon², Robert D. Gerard³, Chou-Long Huang¹, Sarah A. Comerford², Robert E. Hammer⁴, Jay D. Horton², Rui Chen^{1,§}, and Joseph A. Garcia^{1,5,§}

¹Department of Internal Medicine, University of Texas Southwestern Medical Center, 5323 Harry Hines Boulevard Dallas, Texas 75390

²Department of Molecular Genetics, University of Texas Southwestern Medical Center, 5323 Harry Hines Boulevard Dallas, Texas 75390

³Department of Molecular Biology, University of Texas Southwestern Medical Center, 5323 Harry Hines Boulevard Dallas, Texas 75390

⁴Departments of Biochemistry, University of Texas Southwestern Medical Center, 5323 Harry Hines Boulevard Dallas, Texas 75390

⁵Department of Medicine, VA North Texas Health Care System, 4600 South Lancaster Road, Dallas, Texas, 75216

Abstract

Endocrine erythropoietin (Epo), which is synthesized in the kidney or liver of adult mammals, controls erythrocyte production and is regulated by the stress-responsive transcription factor Hypoxia Inducible Factor 2 (HIF-2). We previously reported that the lysine acetyltransferase Cbp is required for HIF-2 α acetylation and efficient HIF-2 dependent *Epo* induction during hypoxia. We now show these processes require acetate-dependent acetyl CoA synthetase 2 (Acss2). In Hep3B hepatoma cells and in Epo-generating organs of hypoxic or acutely anemic mice, acetate levels increase and Acss2 is required for HIF-2 α acetylation, Cbp/HIF-2 α complex formation and recruitment to the *Epo* enhancer, and efficient *Epo* induction. In acutely anemic mice, acetate supplementation augments stress erythropoiesis in an Acss2-dependent manner. In acquired and genetic chronic anemia mouse models, acetate supplementation also increases Epo expression and resting hematocrits. Thus, a mammalian stress-responsive acetate switch controls HIF-2 signaling and Epo induction during pathophysiological states marked by tissue hypoxia.

Keywords

Epo; HIF-2; Cbp; p300; Acss2

Users may view, print, copy, and download text and data-mine the content in such documents, for the purposes of academic research, subject always to the full Conditions of use:http://www.nature.com/authors/editorial_policies/license.html#terms

[§]To whom correspondence should be addressed: Rui Chen, Department of Medicine, UT Southwestern Medical Center, 5323 Harry Hines Blvd., Dallas, Texas 75390-8573; Tel.: (214) 648-1400; FAX: (214) 648-1450; rui.chen@utsouthwestern.edu; Joseph A. Garcia, Department of Medicine, VA North Texas Health Care System, 4600 S. Lancaster Road, Dallas, Texas 75216; Tel.: (214) 857-0240; FAX: (214) 857-0340; joseph.garcia@utsouthwestern.edu.

The authors declare no competing financial interests.

Introduction

Oxygen deprivation induced by hypoxia activates stress responses, one of which for vertebrates is increased red blood cell production or erythropoiesis^{1,2}. The discovery of erythropoietin (Epo), an endocrine growth factor synthesized in the adult kidney and liver, began with elegant physiological experiments demonstrating an erythropoiesis-promoting blood-borne factor, continued with the characterization and purification of the Epo protein, and culminated with cloning of the *Epo* gene³. Mapping of the hypoxia-responsive enhancer region in the *Epo* gene identified a molecular handle subsequently used to purify Hypoxia Inducible Factor 1 (HIF-1)⁴, a sentinel regulator of the mammalian hypoxia response.

HIF-1 is a heterodimeric stress-responsive transcription factor comprised of an oxygen-sensitive alpha subunit and an oxygen-insensitive beta subunit. During hypoxia, HIF-1 α is regulated in a novel manner⁵ through inhibition of two oxygen-dependent modifiers, prolyl hydroxylases (PHDs) that decrease HIF-1 α stability and an asparagine hydroxylase (Factor Inhibiting HIF-1, FIH1) that prevents coactivator/HIF-1 α interactions⁶. Mining of the human genome led to identification of HIF-2 α , the second vertebrate HIF family member⁷⁻⁹. Although structurally similar to HIF-1 α , genetic ablation studies in cells and mice indicated that HIF-2 α , rather than HIF-1 α , is the key regulator of endocrine Epo¹⁰⁻¹⁵.

HIF-2 α undergoes the same oxygen-dependent mechanisms of activation as HIF-1 α , yet HIF-2 α protein increases under hypoxia are relatively modest in some cell lines. This suggests that post-translational mechanisms other than protein stability play an important role in HIF-2 signaling. Indeed, acetylation and deacetylation of HIF-2 α are required for efficient HIF-2 signaling during hypoxia in Hep3B cells and in mice. HIF-2 α acetylation is mediated by the lysine acetyltransferase and coactivator Creb binding protein (Cbp), which also provides a molecular platform for stable Cbp/HIF-2 α complex formation, whereas Sirtuin 1 (Sirt1) is a specific deacetylase for acetylated HIF-2 α ^{10,16}. Notably, the lysine acetyltransferase and coactivator p300, which is closely related to Cbp, does not acetylate HIF-2 α and is a minor component of HIF-2 signaling in Hep3B cells and liver. However, p300 also complexes with HIF-2 α during hypoxia¹⁶. We were interested in further exploring these differences in signaling function for Cbp and p300 in HIF-2 signal transduction.

Results

Acss2 controls HIF-2 signaling in hypoxic cells

We first defined the temporal aspect of HIF-2 α acetylation and Cbp/HIF-2 α complex formation in Hep3B cells. HIF-2 α acetylation and Cbp/HIF-2 α complexes peak early (2 h) whereas p300/HIF-2 α complexes form late (8 h) following hypoxia onset (Fig. 1a,b). Because Cbp/HIF-2 α complex formation requires both Cbp enzymatic (i.e. acetyltransferase activity) and HIF-2 α substrate determinants (i.e. lysine residues) of the acetylation reaction¹⁶, we reasoned that availability of acetyl CoA, the other required substrate in the Cbp acetylation reaction, might control dynamic Cbp/HIF-2 interactions during hypoxia.

Acetyl CoA is synthesized *de novo* by pyruvate dehydrogenase, ATP citrate lyase (Acly), or acetate-dependent acetyl CoA synthetases (Acss). During hypoxia, pyruvate dehydrogenase is inactivated by the HIF-1 target gene pyruvate dehydrogenase kinase^{17,18} whereas Acly, a major source of cytosolic acetyl CoA, remains active¹⁹. Acss1 generates mitochondrial acetyl CoA²⁰ while Acss2 generates cytosolic acetyl CoA²¹⁻²³. Because Acss2 and Acly may reside in the nucleus²⁴, we asked whether their subcellular locations as well as that of Cbp, Sirt1, and HIF-2 α change during hypoxia (Fig. 1c). Acss2 is nuclear-localized during early hypoxia (2 h), coincident with peak acetylation and Cbp/HIF-2 α complex formation, but is cytosolic during late hypoxia (8 h). Acly is mostly cytosolic, Cbp is restricted to the nucleus, and HIF-2 α is present in both the cytosol and nucleus, but their distribution does not change appreciably during hypoxia. Nuclear Sirt1 levels increase during hypoxia, which may be a combination of increases in Sirt1 mass during hypoxia²⁵ as well as an indirect result of passenger effects.

The dynamic behavior of Acss2 subcellular location during hypoxia led us to consider it a candidate acetyl CoA generator for Cbp-mediated HIF-2 α acetylation and therefore a regulator of HIF-2 signaling. We hypothesized that acetate, which is generated by hypoxic cells²⁶, might function as a biochemical cue to activate Acss2. Indeed, acetate levels increase by an early (2 h) hypoxia time-point, and then decline to basal levels (Fig. 1d). As we have shown previously, acetylation of HIF-2 α is dependent upon Cbp and not p300 (Fig. 1e). Knockdown of Acss2, but not of Acss1 or Acly, also eliminates HIF-2 α acetylation as well as Cbp/HIF-2 α complex formation in early hypoxia, which shifts instead to p300/HIF-2 α complex formation (Fig. 1e,f). Finally, Acss2 is required for induction of the HIF-2 target gene *Epo* during hypoxia (Fig. 1g).

We asked whether Acss2 is required for HIF- α or coactivator (p300 or Cbp) recruitment using chromatin immunoprecipitation (ChIP) assays (Supplementary Fig. 1a). HIF-2 α and HIF-1 α recruitment to the *Epo* enhancer is evident during early (2 h) and late (8 h) hypoxia. Acss2 knockdown eliminates HIF-2 α , but not HIF-1 α , recruitment to the *Epo* enhancer as well as Cbp recruitment, but does not affect p300 recruitment. Furthermore, Acss2 knockdown eliminates HIF-2 α recruitment of Cbp during early (2 h) hypoxia as assessed by sequential ChIP, but does not affect HIF-2 α recruitment of p300 during late (8 h) hypoxia (Supplementary Fig. 1b). Conversely, Acss2 knockdown eliminates Cbp recruitment of HIF-2 α during early (2 h) hypoxia, but likewise does not reduce p300 recruitment of HIF-2 α (Supplementary Fig. 1c).

HIF-1 α also regulates *Epo* gene expression in Hep3B cells. However, Acss2 knockdown does not affect HIF-1 α recruitment of Cbp or p300 to the *Epo* enhancer or to the promoter of the HIF-1 selective target gene *Pgk1* during hypoxia (Supplementary Fig. 1d,e). Acss2 knockdown has no effect upon HIF-1 α or HIF-2 α recruitment to a non-hypoxia responsive promoter, *Rpl13a* (Supplementary Fig. 1f). In all chromatin immunoprecipitation experiments, a control immunoprecipitation with a non-specific antibody fails to generate a signal.

Several hypoxia-inducible genes are co-regulated by HIF-1 α and HIF-2 α (*Epo*, *VegfA*, *Pai1*, *Glut1*), by HIF-2 α (*Mmp9*), or by HIF-1 α (*Pgk1*) (Supplementary Fig. 2a–c). For target

genes regulated by HIF-2 α , knockdown of *Acss2*, but not of *Acss1* or *Acly*, blunts induction following hypoxia exposure (Supplementary Fig. 2d). In contrast, induction of a HIF-1 α target gene is unaffected by knockdown of these acetyl CoA generators (Supplementary Fig. 2e).

***Acss2* regulates hypoxia-induced renal *Epo* expression in mice**

We deleted the majority of the *Acss2* gene in mice (Supplementary Fig. 3a). Mixed strain *Acss2* wild-type (WT), but not knockout (KO), mice demonstrate *Acss2* immunoreactivity in renal cortex and medulla as well as in the liver (Supplementary Fig. 3b,c). Following hypoxia exposure, acetate levels in *Acss2* WT and KO kidneys increase by 2 h and remain elevated (Fig. 2a). HIF-2 α isolated from these kidneys is acetylated on lysine residues in an *Acss2*-dependent manner (Fig. 2b). Hypoxia exposure results in HIF-2 α recruitment to the *Epo* enhancer in *Acss2* WT, but not KO, kidneys, and sequential ChIP reveal that Cbp, but not p300, is present when HIF-2 α occupies the *Epo* enhancer in mouse kidney after 2 h hypoxia (Fig. 2c).

We asked if Cbp/HIF-2 α complex formation at the *Epo* enhancer in mice during hypoxia correlates with *Epo* gene expression. Similar to global HIF-2 α KO mice¹¹, *Epo* mRNA synthesis in kidneys of *Acss2* KO mice is markedly blunted after hypoxia exposure (Fig. 2d) as is the increase in plasma *Epo* protein levels that is otherwise observed in *Acss2* WT mice after 16 h of hypoxia exposure (Fig. 2e). However, the short-term duration of hypoxia (16 h) is not sufficient to result in an increase in red blood cell mass other than the initial rise in hematocrit levels during the early (2 h) hypoxia phase, an immediate physiological response²⁷ that is observed in both *Acss2* WT as well as KO mice (Supplementary Fig. 3d).

Acute anemia induces *Acss2*-dependent HIF-2 signaling in mice

To determine if *Acss2*/HIF-2 signaling is relevant under pathophysiological states marked by more prolonged periods of tissue hypoxia, we used phenylhydrazine (PHZ) to induce hemolytic anemia in *Acss2* WT or KO mice²⁸, which results in a comparable degree of severe anemia by 4 days after PHZ injection (Fig. 3a). We noted that the recovery of *Acss2* KO mice takes substantially longer (18 days) than *Acss2* WT mice (9 days), consistent with reduced plasma *Epo* levels observed in *Acss2* KO relative to WT mice at the hematocrit nadir (Fig. 3b).

Acetate levels at the anemia nadir increase to comparable levels in *Acss2* WT and KO kidney and liver (Fig. 3c,d). HIF-2 α acetylation in kidneys and livers of severely anemic *Acss2* WT mice also increases, but is undetectable in *Acss2* KO mice (Fig. 3e,f). Finally, *Epo* mRNA levels are markedly induced in kidneys and livers of anemic *Acss2* WT mice, but are only slightly elevated in these same organs of *Acss2* KO mice (Fig. 3g,h). The absence of *Acss2* has no effect on expression of the HIF-1 target gene *Pgk1* in kidneys or livers of anemic *Acss2* KO versus WT mice (Fig. 3g,h).

An acetate switch regulates Cbp/HIF-2 interactions in cells

We reasoned that acetate generated by hypoxic cells triggers Cbp-mediated HIF-2 α acetylation²⁶. Indeed, HIF-2 α acetylation is increased in cells incubated with early (2 h)

hypoxia conditioned medium or with acetate-supplemented medium, but not with other short chain fatty acid (SCFA) such as butyrate or propionate (Supplementary Fig. 4a, Fig. 4a). HIF-2 α acetylation induced by acetate treatment requires Acss2 and Cbp (Fig. 4b). Similarly, Cbp/HIF-2 α complex formation is observed in cells incubated with early (2 h) hypoxia conditioned medium or with acetate-supplemented medium, but not other SCFA (Supplementary Fig. 4b, Fig. 4c). Stable Acss2-dependent Cbp/HIF-2 α complex formation induced by acetate requires Acss2 as well as Sirt1 and Cbp (Fig. 4d,e), similar to requirements under hypoxia¹⁶. Acetate supplementation results in Acss2 nuclear localization (which is also seen after hypoxia exposure) (Fig. 4f), but the other SCFA do not have this effect. Finally, the loss of acetate-induced HIF-2 α acetylation following Acss2 knockdown is rescued by expression of an shRNA-resistant wild-type, but not mutant, Acss2 cDNA (Fig. 4g).

Exposure of cells to hypoxia, hypoxia-conditioned medium, or exogenous acetate all result in elevated intracellular acetate levels, but only medium of hypoxia and hypoxia-conditioned cells have altered acidity (Supplementary Fig. 4c). Cbp/HIF-2 α complex formation is observed *in vitro* with early (2 h) hypoxia cell extracts and is absent following Acss2 depletion, but is restored with addition of acetyl CoA (Supplementary Fig. 4d). Although normally absent in Acss2-replete, late (8 h) hypoxia cell extracts, Cbp/HIF-2 α complex formation is induced *in vitro* in these extracts by supplementing with either acetyl CoA or acetate and ATP, cofactors required by Acss2²¹ that decrease during hypoxia²⁹ (Supplementary Fig. 4e).

Acss2 signaling in cells requires intact HIF-2 acetylation

To ascertain whether acetate-induced Cbp/HIF-2 α interactions requires HIF-2 α lysine residues acetylated following hypoxia exposure, we exposed knockdown/rescue cells, expressing either rescue HIF-2 α with intact lysine residues that are acetylated during hypoxia (K3) or a HIF-2 α arginine substitution mutant incapable of acetylation (R3)¹⁰, to hypoxia or medium supplemented with each SCFA. K3, but not R3, HIF-2 α is acetylated (Fig. 5a,b) and complexes with Cbp (Fig. 5c,d) during hypoxia or after acetate supplementation. Finally, *Epo* mRNA induction is maximal and is markedly reduced by Acss2 knockdown following hypoxia exposure in K3 HIF-2 α rescue cells (Fig. 5e). In comparison, *Epo* mRNA induction is blunted in R3 HIF-2 α rescue cells following hypoxia exposure and Acss2 knockdown has no effect, consistent with Acss2 action on HIF-2 signaling being mediated through acetylation of the K3 lysine residues.

Acetate facilitates recovery from anemia

To determine if acetate augments recovery from acute anemia, we administered either vehicle (water) or a glyceryl triester of the short chain fatty acids (SCFA) acetate (GTA), butyrate (GTB), or propionate (GTP) to wild-type CD1 mice with phenylhydrazine (PHZ)-induced anemia. To determine if the route of administration influenced its action, we also delivered SCFA by intra-peritoneal injections. Erythropoiesis in acutely anemic wild-type CD1 mice is augmented after supplementation with oral or intra-peritoneal acetate, but not butyrate or propionate (Fig. 6a). Acetate supplementation also speeds recovery from PHZ-

induced anemia in *Acss2* WT, but not KO, mice on a mixed strain genetic background (Fig. 6b).

With respect to changes in hematological parameters, GTA treatment returns hematocrit levels to normal earlier (6 days) than control-treated anemic mice (9 days) (Supplementary Fig. 5a). Despite an initial overshoot, hematocrit levels return to normal within three days even with continued GTA administration. Reticulocyte levels, which increase in acutely anemic mice (day 4 post-PHZ), return to normal faster in GTA- versus vehicle-treated mice (Supplementary Fig. 5b). Increased (kidneys) or prolonged (livers) HIF-2 α acetylation is observed after GTA treatment for acutely anemic CD1 mice (Supplementary Fig. 5c,d).

As for downstream effects on HIF-2 signaling, GTA supplementation results in increased *Epo* mRNA levels in kidneys and livers, which also remain elevated at least 3 days longer than vehicle-treated anemic mice (Supplementary Fig. 6a,b). Nevertheless, soon after hematocrit levels of GTA-treated anemic mice return to normal (Day 10 post-PHZ), *Epo* mRNA levels also return to basal levels in the kidney and liver (Day 13 post-PHZ) and remain so despite continued GTA administration (Days 16 and 20 post-PHZ). Acetate does not augment expression of the HIF-1 target gene *Pgk1* gene in kidney or liver (Supplementary Fig. 6a,b).

We also examined whether acetate supplementation affects erythropoiesis in an acquired chronic anemia model, chronic renal failure (CRF) induced by partial nephrectomy^{30,31}, and a genetic chronic anemia model, double heterozygous (DH) cKit mutant mice^{32,33}. Acetate, but not butyrate or propionate, increases resting hematocrit levels in CRF as well as DH cKit mutant mice (Fig. 6c,d). Although hematocrit levels of CRF as well as DH cKit mutant, but not cKit wild-type, increase (Supplementary Fig. 7a,e), reticulocyte levels only increase for CRF mice, but decrease for DH cKit mutant mice, with acetate treatment (Supplementary Fig. 7b,f). Despite these differences, acetate treatment increases renal *Epo* mRNA levels in both models (Supplementary Fig. 7c,g). Acetate administration results in elevated acetate levels for CRF and DH cKit mutant mice as well as WT cKit mice (Supplementary Figs. 7d,h).

Cyclical acetate treatments of CRF as well as DH cKit mutant results in increased hematocrit levels (Fig. 6e,f) that parallel similar increases in plasma Epo protein (Supplementary Fig. 8a,b), which reverse with cessation of acetate supplementation. Finally, acetate treatment also results in increased acetylated HIF-2 α protein levels in kidneys of CRF and DH cKit mutant mice, but not WT cKit mice (Supplementary Fig. 8c,d).

Discussion

Although exogenous Epo is an effective treatment for anemia, therapies that maintain physiological Epo regulation may reduce deleterious side-effects associated with bolus Epo treatment including hypertension, thrombosis, and possibly accelerated malignancies³⁴⁻³⁶. HIF-2, a key regulator of endogenous *Epo* gene expression, may be a particularly efficacious target. A major finding from this study is that acetate, generated during hypoxia or anemia, is a signaling molecule used by a specific acetyl CoA generator, *Acss2*, to regulate

interactions of HIF-2 α with its selective acetyltransferase and coactivator, Cbp. Recruitment of Cbp/HIF-2 α complexes to the *Epo* enhancer occurs in parallel with Cbp/HIF-2 α complex formation in solution during early hypoxia and also depends upon *Acss2*. Interestingly, at the later phase of hypoxia, Cbp and HIF-2 α remain associated with the *Epo* enhancer, but not with each other, which suggests that the Cbp/HIF-2 α containing enhanceosome assembled at the *Epo* enhancer and likely other HIF-2 target genes undergoes further remodeling as hypoxia progresses.

The exact origin of acetate during hypoxia and anemia is unknown. The liver generates endogenous acetate³⁷ under ambient conditions; a similar process has not been reported for kidney. Kidney as well as liver exhibit zonal hypoxia, which place certain anatomical regions of these organs at risk to further changes in oxygen content^{38,39}. Acetate and acetyl CoA pools in cells rapidly cycle⁴⁰⁻⁴², so perturbations of this cycle during hypoxia and anemia may facilitate transient acetate increases in the kidney and liver⁴³. Histone deacetylation in acidic environments results in acetate release⁴⁴, which may also be relevant. Although increased SCFA levels may impair acetate utilization⁴⁵ or uptake⁴⁶, we find that addition of SCFA besides acetate does not trigger the *Acss2* response. *Acss2* is a proposed acetate generator²⁶, but is likely a minor source in normal cells as acutely hypoxia or anemic *Acss2* WT and KO mice have similar acetate levels in kidney and liver.

Changes in intermediary metabolism during hypoxia initiate *Acss2* activity, but also terminate its action as hypoxia continues. During early (2 h) hypoxia, HIF-2 α acetylation as well as Cbp/HIF-2 α complex formation, which occurs via HIF-2 α binding independent of the carboxy terminal activation domain (CTAD), is stimulated by increased acetate levels and is regulated by *Acss2* in Hep3B cells. During late (8 h) hypoxia, acetate levels return to baseline and ATP levels likely decrease, which limits *Acss2* activity. In addition, Factor Inhibiting HIF-1 (FIH1) is inactive⁴⁷⁻⁴⁹, which means that CTAD-dependent recruitment of p300 can commence.

The molecular and biochemical effects of acetate supplementation include increased HIF-2 α acetylation, *Epo* mRNA levels, and plasma Epo protein levels, which result in an accelerated recovery from acute anemia. Continued acetate treatment has no further effect on hematocrit levels at or close to physiological levels, which indicates proper functioning of the homeostatic mechanisms for hematocrit control under these conditions. Thus, acetate augmentation of HIF-2 signaling in whole animals requires not only *Acss2*, but also the concomitant presence of hypoxemia. Whether this reflects a requirement for inactivation of PHDs or FIH1, or for production of other factors activated during anemia⁵⁰, remains to be determined.

Acetate supplementation may be useful in treating acute anemia in civilian and military scenarios and when patients have faith-based objections to blood transfusions⁵¹. Chronic anemia associated with impaired Epo generation due to reduced HIF-2 signaling may also be impacted by the acetate switch, and may already be unwittingly exploited. End-stage renal disease (ESRD) patients often have anemia as well as blunted *Epo* production^{11,13}, and are dialyzed thrice-weekly with an acetate-containing dialysate that transiently increases plasma acetate levels^{52,53}. ESRD patients transitioned to an acetate-free dialysate⁵⁴ exhibit

increased darbepoetin and iron requirements⁵⁵, consistent with expectations if HIF-2 signaling is impaired. The ability of acetate to increase Epo production in DH cKit mutant mice suggests that acetate may also be effective in treating some genetic disorders associated with impaired Epo, but intact HIF-2, signaling, which may be due to the ability of Epo to influence erythroid progenitor cell fates⁵⁶.

One proposed therapeutic role for acetate supplementation, which may also be mediated by *Acss2*, is in production of acetate-derived lipids²¹ that are used for myelin synthesis in neuropathophysiological states such as traumatic brain injury (TBI)⁵⁷. Notably, TBI, which results in tissue ischemia and hypoxia, results in *Acss2* nuclear localization in astrocytes⁵⁷. HIF-2 is also expressed in astrocytes, where it regulates *Epo* gene expression and may alleviate neurological injury⁵⁸. The broad distribution of *Acss2* in hepatocytes as well as in the renal cortex and medulla may signify an additional physiological role of *Acss2*/HIF-2 signaling, possibly relating to ischemic injury responses regulated by HIF-2^{59,60}. Whether *Acss2* plays a protective role in the injury response of vital organs and, if so, whether the effect of *Acss2* is mediated by anabolic contributions or by signaling events via HIF-2 or other acetylated signal transducers, is a topic for future studies.

Online Methods

Cell culture

We maintained Hep3B cells (Cat. No. HB-8064, ATCC, Manassas, VA) in complete DMEM media (Cat. No. SH30022, HyClone, Logan, UT), 10% fetal bovine serum (FBS; Cat. No. F4135, Sigma) with penicillin (100 U mL⁻¹)/streptomycin (100 µg mL⁻¹) (Cat. No. 15140-148, Gibco BRL, Carlsbad, CA) in a 5% CO₂, 95% air incubator. We assayed cells periodically for mycoplasma. For passaging cells, we added 1 ml 0.25% Trypsin/2.21 mM EDTA/HBSS (Cat. No. 25-052-CI, Corning cellgro, Manassas, VA) to a freshly confluent 10 cm plate and waited 1 min at room temperature. Trypsinized cells from one 10 cm plate were added to complete media (1:3 ratio) and replated into three 10 cm plates. We used cells (unselected or selected) from between 15 and 25 passages in all experiments. For hypoxia treatments (1% O₂, 5% CO₂, 94% N₂), we maintained cells, replaced media with deoxygenated media, and prepared extracts within a humidified environmental chamber (Coy Laboratory Products, Inc., Grass Lake, MI). For short chain fatty acid (SCFA) addition, we added the indicated sterile stocks of SCFA (acetate, propionate, butyrate) to complete medium (final concentration 0.5 mM) and harvested cells after the indicated time under normal oxygen conditions.

Lentiviral generation

We previously described the wild-type (WT) acetylase-sensitive (K3) and acetylase-insensitive (R3; K385R, K685R, K741R) human HIF-2α plasmids^{10,16}. All human HIF-2α rescue cDNA constructs contain a carboxy terminal hemagglutinin A (HA) epitope tag. We generated wild-type (WT) and mutant (MUT) *Acss2* from a mouse *Acss2* cDNA. We constructed MUT *Acss2* cDNA by zipper PCR so that it contains deletions of sequences corresponding to coding exons 3 through 7, and thereby encodes a truncated and non-functional *Acss2* protein not detected by immunoblotting. The rescue HIF-2α and *Acss2*

cDNAs contain silent mutations that confer resistance to siRNA or shRNA directed against the endogenous human protein of interest. All Acss2 constructs contain an amino terminal V5 epitope tag.

The lentiviral knockdown constructs express multiple miR30 shRNAs⁶¹ using Pol II promoters⁶² for efficient knockdown. For knockdown only studies (control and Acss2), lentiviral (LTV) shuttle expression vectors (derivatives of pLenti6/V5-GW/lacZ, Invitrogen that are neomycin instead of blasticidin resistant) harbor a firefly luciferase cDNA followed by a concatamer of four different shRNAs directed against the gene of interest. For knockdown/rescue studies, LTV shuttle expression vectors encode an siRNA/shRNA-resistant mouse Acss2 or human HIF-2 α cDNA followed by an IRES:firefly luciferase:shRNA concatamer cassette (WT and MUT Acss2) or an IRES:DsRed:shRNA concatamer cassette (K3 and R3 HIF-2 α). The seed sequences for the four human ACSS2 shRNA are as follows: 5'-GTAATAGCCATCCTGGTCCCGC-3', 5'-AACTTGGTCACTTGTATTTGT-3', 5'-TGGTATGTGATCTGAGTGGTCT-3', 5'-GTATCCAGGAACTTCTTAAAG-3'. The seed sequences for the four human HIF-2 α shRNA are based on previous siRNAs^{14,63-65} and are as follows: 5'-TTCATACTCCAGCTGTCGCTTA-3', 5'-TAAGTCTATCCGGGCTTACTAC-3', 5'-TCTGTGTCCATGGCGAAGAGCG-3', 5'-ACTGCTATCAAAGATGCTGTTA-3'.

We used the LTV packaging plasmid psPAX2 (Addgene plasmid 12260) and the envelope plasmid pMD2.G (Addgene plasmid 12259) in conjunction with the shuttle expression plasmids to generate lentivirus. We generated concentrated lentiviral stocks from a 10 cm plate of HEK293T cells co-transfected with 3 μ g LTV shuttle expression vector, 2.25 μ g plasmid psPAX2 and 0.75 μ g pMD2G using Lipofectamine 2000 (Cat. No. 11668019, Invitrogen) using Lenti-X Concentrator (Cat. No. 631232, Clontech). We aliquoted the virus immediately and stored at -80° C until use.

Stable cell line generation

The day before transduction, we plated 2×10^5 Hep3B cells per well in 1 mL complete culture medium overnight in a 6-well plate. On the day of transduction, we replaced media with 1 mL of complete medium with 10 μ g mL⁻¹ polybrene (Cat. No. 107689, Sigma, St. Louis, MO). We thawed lentiviral particles to room temperature, mixed gently, and added to Hep3B cells (MOI=30). After 12 h, we replaced culture medium with 2 mL of complete medium containing 400 μ g mL⁻¹ G418 (Cat. No. SV3006901, HyClone), and replaced it every 2 days until one week after all control cells died. We maintained the initially positive-selected cells in 100 μ g mL⁻¹ G418 for 2 weeks, harvested into a smaller dish until confluent, split cells at 1:3 ratio and grew for at least ten passages under drug selection, and then froze the cells down until use. For experiments, we thawed cells, maintained cells in 100 μ g mL⁻¹ G418, split cells 1:3 for at least three passages when growing exponentially, trypsinized cells lightly at room temperature, and used cells in actual experiments without drug selection when freshly confluent. We used cells fifteen to twenty-five passages from initial drug selection.

siRNA/shRNA knockdown

For transient siRNA knockdown experiments, we used the following siRNAs (Thermo Fisher Scientific, Lafayette, CO): non-targeting control (Cat. No. D-001810-10-20), ACSS1 (Cat. No. L-008549-01-0005), ACSS2 (Cat. No. L-010396-00-0005), ACLY (Cat. No. L-004915-00-0005), p300 (Cat. No. L-003486-00-0005), CBP (Cat. No. L-003477-00-0005), SIRT1 (Cat. No. L-003540-00-0005), HIF-1 α (Cat. No. 004018-00-0005), HIF-2 α (Cat. No. L-004814-00-0005). We transfected siRNA into Hep3B cells using DharmaFECT1 (Cat. No. T-2001-03, Thermo Fisher Scientific) as quadruplicate biological replicates in a 12-well plate with three wells subsequently pooled for use in mRNA analyses and one well used for protein analyses.

For transient lentiviral transduction knockdown (control, ACSS2)/rescue (WT and MUT Acss2) experiments, we added 100 μ L of concentrated lentiviral preparations to a 60 mm Hep3B plate, waited 6 h, then changed the medium to complete medium. After an additional 36 h, we performed the indicated experiment. For stable lentiviral transduction knockdown (control, HIF-2 α)/rescue (K3 and R3 HIF-2 α) experiments, we thawed, grew, split, and used cells as described above. Experiments were performed without drug selection as described above.

Immunoblotting

We used 20 μ g Hep3B whole cell extracts, 20 μ g Hep3B nuclear or cytosolic extracts, and 10 μ g mouse kidney or liver extracts for immunoblotting^{10,16}. To prepare whole cell extracts from Hep3B cells, we used CytoBuster protein extraction reagent (Cat. No. 71009, Novagen, Gibbstown, NJ) with 1 \times protease inhibitor cocktail (Cat. No. P8340, Sigma, St. Louis, MO) and 1 mM PMSF (phenylmethylsulfonyl fluoride) (Cat. No. P7626, Sigma), and stored extracts at -80°C until use. To prepare nuclear extracts from Hep3B cells, we used NE-PER[®] nuclear and cytoplasmic extraction reagents (Cat. No. 78833, Pierce, Rockford, IL) according to the manufacturer's protocol, and stored extracts at -80°C until use. To prepare tissue extracts from liver or kidney, we used CytoBuster protein extraction reagent with 1 \times protease inhibitor cocktail and 1 mM PMSF, and stored extracts at -80°C until use.

We used antibodies raised against the following antigens: human p300 (1:500 dilution; Cat. No. sc-584, Santa Cruz Biotechnology, Santa Cruz, CA), human CBP (1:500 dilution; Cat. No. 7389, Cell Signaling Technology, Danvers, MA), human SIRT1 (1:1,000 dilution; Cat. No. 07131, EMD Millipore, Billerica, MA), human ACLY (1:1,000 dilution; Cat. No. 3378, Cell Signaling Technology), human ACSS1 (1:1,000 dilution; Cat. No. SAB1400745, Sigma), human ACSS2 (1:500 dilution; Cat. No. ab66038, Abcam, Cambridge, MA), human HIF-1 α (1:1,000 dilution; Cat. No. 610958, BD Biosciences), human HIF-2 α (1:1,000 dilution; Cat. No. NB10-132, Novus Biologicals, Littleton, CO), α -tubulin (1:10,000 dilution; Cat. No. T9026, Sigma), TATA-binding protein (TBP) (1:1,000 dilution; Cat. No. sc-204, Santa Cruz Biotechnology), acetyl-lysine (1:1,000 dilution; Cat. No. 9814, Cell Signaling Technology), HA epitope (1:5,000 dilution; Cat. No. H9658, Sigma), V5 epitope (1:10,000 dilution; Cat. No. R960-25, Invitrogen).

Acetate measurements

For cellular acetate measurements, we plated Hep3B cells at 80% confluency as triplicate biological replicates in 60 mm plates and grew them overnight in an incubator within the hypoxia workstation until the indicated time-point. At the time of harvest, we aspirated off media, added 1 mL ice-cold 0.1 N HCl and scraped cells. We transferred the lysate from each plate to an ice-cold microfuge tube and pelleted the cellular debris at 14,000 rpm, 4 °C, 10 min. We transferred 0.9 mL supernatant to a new, ice-cold microfuge tube, and then adjusted the pH to 6.5-7.0 with 5 N NaOH. We determined acetate concentrations from freshly prepared extracts in duplicates using the Megazyme Acetic Acid Rapid Kit (Cat. No. K-ACETRM, Megazyme, Ireland).

For hypoxic mouse kidneys, we exposed *Acss2* wild-type and knockout mice to room air (21% O₂) or hypoxia (6% O₂) for 2 h and then euthanized under normoxic or hypoxic air mixtures to harvest kidney samples. For anemic mouse kidneys and livers, we euthanized under normoxic air mixtures to harvest kidney samples. To measure tissue acetate levels, we placed (~0.1 g) weighed, freeze-clamped, powdered tissue into a cold microfuge tube on dry ice, and slowly added 500 µL ice-cold 1 N perchloric acid. We slowly thawed the samples on ice and then followed with homogenization (PowerGen 700D, Fisher Scientific). We pelleted the homogenate at 14,000 rpm, 4 °C, 10 min. We transferred 0.5 mL supernatant to a new, ice-cold microfuge tube, and then adjusted the pH to 6.5–7.0 with 10 N NaOH. We incubated the extract on ice for 30 min to precipitate proteins, and then centrifuged at 14,000 rpm, 4 °C, 10 min. We transferred the supernatant to a new tube and assayed fresh as single measurements described above and normalized to the weight of tissue used.

Endogenous HIF-2 α acetylation/cells

We cultured Hep3B cells in a single 100 mm plate in complete medium supplemented with 5 µM sirtinol plus 10 mM NAM for 6 h under either normoxia or hypoxia. For acetylation assay using whole cell extracts, we lysed cells with CytoBuster protein extraction reagent supplemented with 1× protease inhibitor cocktail, 1 mM PMSF, 10 mM NAM, and 5 µM sirtinol. For acetylation assay with nuclear or cytosolic protein extracts, we fractionated cells and extracted the nuclear protein using a kit (Cat. No. 40010, Active Motif, Carlsbad, CA) supplemented with 1× protease inhibitor cocktail, 1 mM PMSF, 10 mM NAM, and 5 µM sirtinol. To immunoprecipitate endogenous HIF-2 α , we incubated extracts with a monoclonal human HIF-2 α antibody (Cat. No. NB100-132, Novus Biologicals) for 1 h and then immunoprecipitated using magnetic protein G beads (Cat. No. 54002, Active Motif). We immunoblotted for endogenous HIF-2 α or acetyl lysine as described^{10,16}.

For short chain fatty acid (SCFA) experiments, we cultured a single 60 mm plate of Hep3B cells for 2 h in complete medium with 5 µM sirtinol plus 10 mM NAM under normoxia, and then incubated for 4 h with medium containing vehicle, sodium acetate, sodium propionate, or sodium butyrate with 5 µM sirtinol plus 10 mM NAM. For conditioned media experiments, we cultured a single 60 mm plate of Hep3B cells for 4 h under normoxia in complete medium supplemented with 5 µM sirtinol plus 10 mM NAM, and then incubated for an additional 2 h under either normoxia (control media) or hypoxia (conditioned media).

We replaced 2 mL of cell media of normoxia-maintained Hep3B cells (cultured for 4 h in complete medium with 5 μ M sirtinol plus 10 mM NAM) with either 2 mL of control or conditioned media, and incubated the cells for 2 h. We then prepared whole cell extracts for immunoblotting of endogenous HIF-2 α or acetyl lysine.

For transient transfection siRNA knockdown experiments, we first transfected Hep3B cells in a single 60 mm plate with siRNA, maintained the transfected cells in complete medium for 42 h under normoxia, changed medium to complete medium with 5 μ M sirtinol plus 10 mM NAM, maintained cells for another 6 h under normoxia, exposed cells to the indicated condition, and then prepared whole cell extracts for immunoblotting of endogenous HIF-2 α or acetyl lysine.

For lentiviral knockdown (control, *Acss2*) and knockdown/rescue (WT and MUT *Acss2*) experiments, 36 h after changing from polybrene-containing medium to complete medium (42 h after initial viral transduction), we cultured a single 60 mm plate of Hep3B cells for 2 h in complete medium with 5 μ M sirtinol plus 10 mM NAM under normoxia, and incubated for 4 h with medium containing vehicle or sodium acetate with 5 μ M sirtinol plus 10 mM NAM. We then prepared whole cell extracts for immunoblotting of endogenous HIF-2 α or acetyl lysine.

Ectopic HIF-2 α acetylation/cells

We housed a single 60 mm plate of stably transformed Hep3B cells expressing WT K3 or R3 HIF-2 α under normoxia for 6 h in complete medium containing 5 μ M sirtinol plus 10 mM NAM, and then we transferred cells to either normoxia or hypoxia for the indicated period. At the end of the incubation period, we lysed cells with CytoBuster protein extraction reagent supplemented with 1 \times protease inhibitor cocktail, 1 mM PMSF, 10 mM NAM, and 5 μ M sirtinol. We purified ectopic HIF-2 α :HA by HA-agarose pulldown, and then first immunoblotted using antibody recognizing acetylated lysine and second immunoblotted using antibody recognizing the HA epitope as previously described^{10,16}.

Endogenous HIF-2 α acetylation/mice

We lysed mouse liver (~50 mg) or kidney samples (~100 mg) at the time of harvest in 0.5 mL CytoBuster protein extraction reagent supplemented with 1 \times protease inhibitor cocktail, 1 mM PMSF, 10 mM NAM, and 5 μ M sirtinol. We incubated protein extract (500 μ g) with a monoclonal human HIF-2 α antibody for 1 h to bind endogenous HIF-2 α protein and immunoprecipitated the complex using magnetic protein G beads (Cat. No. 54002, Active Motif). We then immunoblotted for endogenous HIF-2 α or acetyl lysine as described^{10,16}.

Immunoprecipitation experiments/cells

We immunoprecipitated endogenous HIF-2 α proteins from a single 100 mm plate of Hep3B cells using a Universal Magnetic Co-IP kit (Cat. No.54002, Active Motif) according to the manufacturer's protocol. We first incubated whole cell extracts (500 μ g) with magnetic protein G beads. We then incubated the cleared supernatants with antibodies to HIF-2 α (endogenous) or HA (rescue HIF-2 α protein), or with normal mouse (Cat. No. sc-2025, Santa Cruz Biotechnology) IgG, for 2 h before addition of magnetic protein G beads. After

binding, we pelleted beads by centrifugation. After washing, we eluted the immunoprecipitated proteins and immunoblotted with antibodies to human p300 (1:500 dilution; Cat. No. sc-584, Santa Cruz Biotechnology), human CBP (1:500 dilution; Cat. No. 4772, Cell Signaling Technology), or HIF-2 α (1:1,000 dilution; Cat. No. NB100-132, Novus Biologicals).

***In vitro* immunoprecipitation experiments/extracts**

We first transfected Hep3B cells in a single 100 mm plate with siRNA, waited 48 h, exposed cells to the indicated condition, and prepared whole cell extracts using a Universal CoIP Kit (Cat. No. 54002, Active Motif) as described¹⁰. For hypoxia samples, we performed all initial extract preparations in the hypoxia workstation. For all subsequent *in vitro* experiments, we performed manipulations under normal oxygen conditions. We next added acetyl CoA (final concentration 50 μ M; Cat. No. A2056, Sigma), ATP (final concentration 100 μ M; Cat. No. FLAAS-1VL, Sigma), or acetate (final concentration 50 μ M; Cat. No. A2056, Sigma) to 50 μ l whole cell extract and incubated the extract at 30 °C for 30 min. We then immunoprecipitated endogenous HIF-2 α and performed immunoblotting for HIF-2 α , CBP, or p300 as described^{10,16}.

Real-time PCR analyses

We determined the expression of endogenous *Epo*, *VegfA*, *Pai1*, *Mmp9*, *Glut1*, *Pgk1*, and *cyclophilin B* from a single pooled sample made from three individually transfected wells (biological replicates) of Hep3B cells in a 12-well plate for each condition or of endogenous *Epo* and *cyclophilin B* from the indicated number of individual mouse organs (biological replicates). We generated cDNA by reverse transcription of total RNA followed by real-time PCR analysis (rtRTPCR) performed and measured in triplicate (three technical replicates) using human or mouse specific primer pairs as previously described^{10,16}. We used the following human rtRTPCR primer pairs: *Epo* (forward) 5'-GAGGCCGAGAATATCACGACGGG-3', *EPO* (reverse) 5'-TGCCCGACCTCCATCCTTCCAG-3'; *VEGFa* (forward) 5'-AGTAGCTGCGCTGATAGACATCCATGA-3', *VEGFA* (reverse) 5'-CACCCATGGCAGAAGGAGGAGGGCAGAA-3'; *PAI1* (forward) 5'-ATTC AAGCAGCTATGGGATTCAA-3', *PAI1* (reverse) 5'-CTGGACGAAGATCGCGTCTG-3' [PrimerBank ID 10835159a2]; *MMP9* (forward) 5'-GGGACGCAGACATCGTCATC-3', *MMP9* (reverse) 5'-TCGTCATCGTCGAAATGGGC-3' [PrimerBank ID 4826836a2]; *GLUT1* (forward) 5'-CTTTTCTGTTGGGGGCATGAT-3', *GLUT1* (reverse) 5'-CCGCAGTACACACCGATGAT-3' [PrimerBank ID 5730051a2]; *Pgk1* (forward) 5'-TTAAAGGGAAGCGGGTCGTTA-3', *Pgk1* (reverse) 5'-TCCATTGTCCAAGCAGAATTTGA-3'; *Cyclophilin B* (forward) 5'-ATGTGGTTTTTCGGCAAAGTTCTA-3', *Cyclophilin B* (reverse) 5'-GGCTTGTCGGGCTGTCT-3'. We used the following mouse rtRTPCR primer pairs: *Epo* (forward) 5'-GAGGCAGAAAATGTCACGATG-3', *Epo* (reverse) 5'-CTTCCACCTCCATTCTTTTCC-3'; *Pgk1* (forward) 5'-CTCCGCTTTCATGTAGAGGAAG-3', *Pgk1* (forward) 5'-GACATCTCCTAGTTTGGACAGTG-3'; *Cyclophilin B* (forward) 5'-

ATGTGGTTTTTCGGCAAAGTTCTA-3', *Cyclophilin B* (reverse) 5'-GGCTTGTCCTCCGGCTGTCT-3'.

Chromatin Immunoprecipitation (ChIP) Assays/cells

For each Hep3B sample analyzed in ChIP experiments, we seeded three individual 150 mm plates with 2×10^6 Hep3B cells per plate 48 h prior to use, exposed the cells to normoxia or hypoxia, and then pooled the three biological replicates together for chromatin preparations. We prepared a separate 150 mm plate in parallel for use in assessment of EPO induction after hypoxia exposure, which was confirmed by real-time RT-PCR, and for protein analyses. We performed sequential chromatin immunoprecipitation assays (Re-ChIP) using the Re-ChIP-IT™ magnetic chromatin re-immunoprecipitation kit (Cat. No. 53016, Active Motif). We used the following antisera for the first chromatin immunoprecipitation reaction: normal mouse IgG (1–2 mg mL⁻¹; Cat. No. 2027, Santa Cruz Biotechnology, Inc.), normal rabbit IgG (1–2 mg mL⁻¹; Cat. No. NI01, EMD Chemicals, Inc., Gibbstown, NJ), anti-human HIF-1 (250 µg mL⁻¹; No 610958, BD Biosciences), anti-human EPAS1 (1 mg mL⁻¹; Cat. No. NB 100-132, Novus Biologicals), anti-human p300 (2 mg mL⁻¹; Cat. No. sc-584, Santa Cruz Biotechnology), or anti-human CBP (2 mg mL⁻¹; Cat. No. 7389, Cell Signaling Technology). We used the following antisera for the second chromatin immunoprecipitation reaction: anti-human p300 (2 mg mL⁻¹; Cat. No. sc-584, Santa Cruz Biotechnology), anti-human CBP (2 mg mL⁻¹; Cat. No. 7389, Cell Signaling Technology), anti-human HIF-1 (250 µg mL⁻¹; Cat. No. 610958, BD Biosciences), or anti-human EPAS1 (1 mg mL⁻¹; Cat. No. NB 100-132, Novus Biologicals).

After the sequential ChIP, we analyzed the precipitated genomic DNA by quantitative PCR using an Applied Biosystems ABI Prism 7000 thermocycler (Applied Biosystems, Foster City, CA) and Power SYBR Green Master Mix (Cat. No. 4367659, Applied Biosystems) with the following human *EPO* enhancer primers: 5'-CTCTGTCCCACTCCTGGCAGCAGTG -3' (forward) and 5'-CCTTGATGACAATCTCAGCGCACTG-3' (reverse), or human *PGK1* promoter primers: 5'-GGATCTTCGCCGCTACCCTTGTG -3' (forward) and 5'-CTATTGGCCACAGCCCATCGCGGTC -3' (reverse), or human *RPL13A* promoter primers: 5'-GAGGCGAGGGTGATAGAG -3' (forward) and 5'-ACACACAAGGGTCCAATTC -3' (reverse). We normalized captured genomic DNA to input material, and compared the normoxic and hypoxic samples.

Chromatin Immunoprecipitation (ChIP) Assays/mice

For mouse ChIP experiments, we exposed 4 *Acss2* wild-type and 4 knockout mice to room air (21% oxygen) or hypoxia (6% oxygen) for 2 h as we have done previously^{10,11}, and then euthanized the mice under normoxic or hypoxic air mixtures to harvest the kidney samples. We minced 30 mg of fresh tissue to 1–3 mm³, transferred tissue into 10 mL of PBS plus 100 µL 1× protease inhibitor cocktail (Cat. No. P8340, Sigma), added formaldehyde (final concentration 1%), and rotated tubes at room temperature for 15 min. We stopped cross-linking with fresh glycine (final concentration 0.125 M). After 5 min at room temperature, we pelleted the samples in a centrifuge at 420 g at 4 °C, washed once with cold PBS plus protease inhibitors, and then repelleted. We resuspended the washed pellet in 1 mL of PBS

on ice and ground the tissue using a micro-tissue grinder on ice. We pelleted cells again as above at 4 °C. We carried out ChIP using the ChIP-IT™ Express Magnetic assay kit (Cat. No. 53009, Active Motif). For sequential ChIP experiments, we prepared and analyzed *Acss2* wild-type and knockout kidney samples using the reagents as described above. We analyzed precipitated genomic DNA by quantitative PCR in triplicate measurements for each sample using the following mouse *Epo* enhancer primers: 5'-CTGTACCTCACCCCATCTGGTC -3' (forward) and 5'-CCCAGCTCACTCAGCACTTGTCC -3' (reverse), or mouse *Pgk1* promoter primers: 5'-GGCATTCTGCACGCTTCAA -3' (forward) and 5'-GAAGAGGAGAACAGCGCGG -3' (reverse). We normalized captured genomic DNA to input material and compared the normoxic and hypoxic samples.

Generation of *Acss2* knockout mice

For *Acss2* knockout (KO) mouse studies, we created *Acss2* KO mice using SM-1 mouse embryonic stem cells (129S6/SvEvTac) by disruption of the *Acss2* gene using a targeting construct containing ~5 kb of intronic DNA just upstream of exon 3 and ~1 kb of DNA just downstream of exon 16 separated by a neomycin resistance drug cassette, Pol II-neo-Bovine pA and two copies of HSV-TK outside the 3' end of the targeting construct⁶⁶. The gene targeting and creation of chimeric mice were previously described⁶⁷. We mated chimeric founder mice with C57Bl/6J mice to generate mixed strain heterozygous *Acss2* progeny, which maintained by random matings of heterozygous *Acss2* mice for more than 10 generations. We then crossed the line with C57Bl/6J/129 F1 hybrid mice and maintained on this mixed background for more than 10 generations. We generated mixed strain *Acss2* wild-type (WT) and homozygous knockout (KO) mice from matings of heterozygous *Acss2* mice, which were fertile and used to generate progeny for study use. We maintained mice under standard conditions (7 am/7 pm light/dark cycle) in the UTSWMC animal facilities and fed them *ad lib* with standard chow. The UTSWMC Institutional Animal Care and Use Committee approved all experiments.

Mouse experiments/hypoxia exposure

For hypoxia exposure experiments, we examined equal numbers of 10–11 week old wild-type versus homozygous *Acss2* knockout mice under normoxia (room air, 21% oxygen) or the indicated period of short-term hypoxia exposure (6% oxygen; 0.5, 2, 8 16 h) we have done previously^{10,11}. After treatment, we euthanized mice and harvested kidneys for further characterization. We derived baseline hematocrits from normoxia mice. The UTSWMC Institutional Animal Care and Use Committee approved all experiments.

Mouse experiments/Phenylhydrazine (PHZ)-induced anemia

For *Acss2* knockout mice anemia studies, after measuring baseline hematocrits via the tail vein, we injected 3–4 mo *Acss2* wild-type (WT) or knockout (KO) mice (6 mice per group) with 40 mg kg⁻¹ of phenylhydrazine hydrochloride (PHZ; Cat. No. 114745-5G, Sigma) in normal saline or an equal volume of normal saline two times at 24 h intervals, with equal numbers of male (4) and female (2) mice in each group. We bled mice from tails to measure hematocrits 48 h (day 2) and 96 h (day 4; nadir) after the initial PHZ injection. For acetate

supplements, we administered 400 μL of a sterile 0.5 M stock solution of either PBS (vehicle) and sodium acetate/PBS (A, Ac, NaAc) as a single dose at approximately 9 am on the day of treatment by intra-peritoneal injection to PHZ-treated WT or KO Acss2 mice (three mice per group, all males) with hematocrits between 21% and 25% starting on day 4 following the initial PHZ dose. We measured hematocrits every 3 days beginning on day 4 after the initial PHZ injection, and on the final day of euthanasia when we euthanized mice for organ harvesting. The UTSWMC Institutional Animal Care and Use Committee approved all experiments.

For CD-1 mice/acetate treatment acute anemia studies, we injected 7–8 week old (20–24 g) CD1 female mice intra-peritoneal (Charles River Laboratories; Wilmington, MA) with 60 mg kg^{-1} of PHZ in normal saline (PHZ) or normal saline (control) two times at 24 h intervals. We bled mice from the tails to measure hematocrits 96 h (day 4) after the initial injection. For the PHZ treatment group, we first selected mice according to an acceptable range of anemia ($\sim 21\text{--}24\%$). We then subdivided mice into groups of 5 mice (plus up to 3 extra mice to allow for losses or harvesting of mice during the protocol) for every collection day with similar starting mean hematocrit levels for each group (see Supplemental Table 1). We gavaged anemic mice per os (po) with vehicle (water), glyceryl triacetate (GTA; 90 $\mu\text{L}/25$ gm body weight; Cat. No. W200700, Sigma-Aldrich Chemicals, Saint Louis, MO) glyceryl tributyrate (GTB; 140 $\mu\text{L}/25$ gm body weight; Cat. No. W222305, Sigma), or glyceryl tripalmitate (GTP; 115 $\mu\text{L}/25$ gm body weight; Cat. No. W328618, Sigma) using a 20 gauge stainless steel animal feeding tube (Cat. No. FTSS-20S-25, Instech Solomon). We performed gavage once a day in the morning from day 4 to day 20 until euthanasia. We euthanized mice and harvested organs for further characterization on day 4, 7, 10, 13, 16, and 20 after the initial PHZ injection, corresponding to day 0, 3, 6, 9, 12, and 16 of gavage. We gave a control treatment group (solvent injection) - which had approximately equal baseline hematocrits ($\sim 49\%$) - acetate (GTA) or vehicle (water) by oral gavage once a day starting on day 4 following solvent injection and we harvested the mice on day 4, 7, 10, 13, 16, and 20 after the initial solvent injection. We noted no differences in hematocrit levels in this control group (data not shown).

For intra-peritoneal (ip) short chain fatty acid (SCFA) treatments, we prepared a sterile 0.5 M stock solution of each SCFA using sterile PBS and filter-sterilized using a 0.2 μM filter (Cat. No. 190-2520, Thermo Scientific). We injected mice intra-peritoneally with the indicated SCFA/PBS or vehicle (sterile PBS alone) solution. We did not blind investigators as to PHZ or gavage treatments because of institutional animal monitoring requirements, although we performed harvesting and blood draws of mice using only eartag identifiers. The UTSWMC Institutional Animal Care and Use Committee approved all experiments.

Mouse experiments/chronic renal failure (CRF)

Prior to nephrectomy, we collected blood by eye bleeds for baseline hematocrit, plasma creatinine, and blood urea nitrogen (BUN). We performed 5/6 nephrectomy on wild-type CD-1 female mice ($n=49$, 6 wo, 25–28 g; Charles River, Strain Code 022)³⁰. Four weeks after nephrectomy, we again collected blood and plasma from the surviving mice ($n=33$) for analysis. We excluded CRF mice with hematocrits less than 21% or greater than 25%. We

supplemented three groups of CRF mice - which exhibited approximately equal composite hematocrit, plasma creatinine, and plasma BUN means (see Supplemental Table 1) - with vehicle alone (Group A), cyclical acetate or vehicle (Group B), or a single week of short chain fatty acids (Group C). For supplements, we administered 400 μ L of a sterile 0.5 M stock solution of either PBS (vehicle), sodium acetate/PBS (A, Ac, NaAc), sodium butyrate/PBS (B, Bu, NaBu), or sodium propionate/PBS (P, Pr, NaPr) by thrice-weekly (Monday, M/Wednesday, W/Friday, F) intra-peritoneal single dose injections at approximately 9 am on the day of treatment for the indicated periods. We obtained hematocrits via eye bleeds on the Monday of each week, prior to supplement or as indicated. After completion of the treatment protocol, we harvested blood and kidneys for further characterization after euthanasia. The UTSWMC Institutional Animal Care and Use Committee approved all experiments.

Mouse experiments/double heterozygous cKit mutant

We obtained double heterozygous (DH) cKit mutant mice (Kit^W/Kit^{W-v}) on a WBB6 F1 hybrid background (Jackson Laboratories, Stock No. 100410) and wild-type controls from the same colony and housed under standard conditions. For treatments, we obtained baseline hematocrits via eye bleeding, and then we administered 400 μ L of a sterile 0.5 M stock solution of either PBS (vehicle), sodium acetate/PBS (A, Ac, NaAc), sodium butyrate/PBS (B, Bu, NaBu), or sodium propionate/PBS (P, Pr, NaPr) for the indicated periods as thrice-weekly (Monday, M/Wednesday, W/Friday, F) intra-peritoneal injections as a single dose at approximately 9 am on the day of treatment. After completion of the treatment protocol, we harvested blood and kidneys for further characterization after euthanasia. The UTSWMC Institutional Animal Care and Use Committee approved all experiments.

Immunohistochemistry

We fixed tissues used for immunohistochemical analyses in 10% neutral-buffered formalin, paraffin-embedded, and sectioned at 5 μ m. We mounted sections on poly-L-lysine coated glass slides, baked at 56 °C for 30 min, deparaffinized in xylene, and rehydrated through graded alcohols. We quenched endogenous peroxidase activity by incubating slides in 3% hydrogen peroxide (Cat. No. H1009-100ML, Sigma) in deionized water for 30 min and rinsing in deionized water twice for 5 min. For Acss2 antibody (Cat. No. 3658, Cell Signaling Technology) staining, we incubated slides with the BD Retrieval A working solution (Cat. No. 550524, BD Biosciences, San Jose, CA) and heated to ~90 °C (193 °F) in a microwave oven for 10 min, followed by slow cooling to room temperature over 60 min. We then rinsed slides twice with deionized water, and next rinsed once with PBS for 10 min. We blocked non-specific binding by incubation with 10% goat serum (Cat. No. S-1000, Vector Laboratories, Burlingame, CA) in PBS for 60 min. Next, we incubated slides with Acss2 primary antibody (1:150 in 10% goat serum with PBS) overnight at 4 °C and then with biotin-conjugated goat anti-rabbit IgG (1:500 in 10% goat serum with PBS) for 2 h. After rinsing in PBS, we incubated slides with HRP conjugated streptavidin (1:750 in 10% goat serum with PBS) for 60 min at room temperature. After rinsing in PBS, we visualized immunoreactive deposits by incubation with 3'-amino-9-ethylcarbazole (Cat. No. 00-2007, Invitrogen) for 10 min (kidney sections) or 15 min (liver sections). Finally, we

counterstained slides with hematoxylin QS (Cat. No. H-3404, Vector Laboratories) for 2 min, and cover-slipped using Aqua-Polymount (Cat. No. 18606, Polysciences, Inc.).

Plasma Epo protein measurements

To harvest plasma, we mixed 200 μ L eye blood with 7.8 μ L heparin (Cat. No. NC9593879, Fisher Scientific), incubated 30 min on ice, and spun down at 14,000 g for 10 min. We then removed the supernatant and stored in -80°C until analysis. For plasma Epo protein measurements, we assayed 25 μ L of plasma in duplicates using a Mouse Erythropoietin Quantikine ELISA Kit (Cat. No. MEP00B, R&D System).

Plasma chemistry, hematocrit, and reticulocyte measurements

To measure creatinine and blood urea nitrogen (BUN), we divided 50 μ L plasma into two aliquots and measured in duplicates using a Vitros 250 Chemistry System machine (Ortho-Clinical Diagnostics, Inc.) with VITROS CREA or VITROS BUN/UREA slides running on VITROS Chemistry System performed in the UTSWMC Mouse Metabolic Phenotyping Core Facility.

We obtained spun hematocrits from tail-vein or eye bleeds¹². For reticulocyte measurements, we obtained dried blood smears and stained using new methylene blue solution (0.5 g new methylene blue, 1.4 g potassium oxalate, 0.8 g sodium chloride brought to 100 mL using deionized water and filtered using a 0.45 μ m filter). We stained slides for 10 min, rinsed three times in PBS for 5 min each, and then cover-slipped. We counted cells and reticulocytes in three fields chosen at random (40 \times magnification, \sim 500 to 1,000 cells/field) and summed to determine reticulocyte percentage.

Statistical analyses

The observations regarding acetate and *Acss2* in HIF-2 signaling and *Epo* regulation are novel. As we collected molecular and biochemical data for the role of acetate/*Acss2* switch in regulation of HIF-2 signaling and *Epo* regulation in Hep3B cells, we anticipated a similar role for the acetate/*Acss2* switch in mice. Therefore, we considered the mouse experiments as exploratory studies aimed at identifying a meaningful biological role for acetate and *Acss2* in HIF-2 signaling and *Epo* regulation. Accordingly, we were interested in sample sizes that allowed for detection of a very large effect size^{68,69}. We used one-way statistical testing in anticipation of similar results in mice as we noted in Hep3B cells. We chose $\alpha=0.10$ and $\beta=0.20$ as an acceptable Type I and Type II statistical error, respectively, and therefore set power=0.80. Given the small sample size, we performed testing for both normal as well as non-normal distributions, but only report statistics for normal distributions.

We used GraphPad Prism and StatPlus to analyze data by t test or Mann-Whitney for two group comparisons and by one-way or two-way ANOVA for multiple comparisons followed by Tukey's or Dunnett's correction to provide coverage for Type I statistical error. When one group was used as a control to compare to all other groups, we used Dunnett's correction to minimize the effect of multiple comparisons on the p-value. Where all comparisons were performed, we used Tukey's correction.

Supplementary Material

Refer to Web version on PubMed Central for supplementary material.

Acknowledgments

We thank R. Hogg, A. Das, J. Colunga, S. Nystrom, and E. Ballard for technical assistance. We thank D. Trono, École polytechnique fédérale de Lausanne for making the lentiviral packaging and envelope plasmids available to us through Addgene.

M.X., J.S.N., and R.C. conducted the majority of experiments; J.L. and R.D.G. contributed to the protein and viral studies; J.X. and C.-L.H. generated the partial nephrectomy chronic renal failure mice and assisted in their evaluation; H.W., Y.A.M., J.D.H. and R.E.H. generated the *Acss2* KO mouse model; S.A.C. and R.E.H. developed as well as assisted with *Acss2* immunohistochemistry studies; J.A.G. wrote the manuscript and prepared the figures; M.X., J.S.N., R.C., R.D.G., J.X., C.-L.H., J.D.H., S.A.C. and R.E.H. assisted with editing of the manuscript; R.C. and J.A.G. designed and supervised the project as well as analyzed the data.

These studies were supported by funds provided by the US Department of Veterans Affairs (I01BX000446 - J.G.), and the US National Institutes of Health (HL108104 - J.G.; HL20948 - J.H.; DK79328 - C.-L.H.).

References

1. Bunn HF, Poyton RO. Oxygen sensing and molecular adaptation to hypoxia. *Physiological Reviews*. 1996; 76:839–885. [PubMed: 8757790]
2. Richalet JP. Oxygen sensors in the organism: examples of regulation under altitude hypoxia in mammals. *Comparative Biochemistry & Physiology, Part A Physiology*. 1997; 118:9–14.
3. Koury MJ. Erythropoietin: the story of hypoxia and a finely regulated hematopoietic hormone. *Exp Hematol*. 2005; 33:1263–1270. [PubMed: 16263408]
4. Wang GL, Jiang BH, Rue EA, Semenza GL. Hypoxia-inducible factor 1 is a basic-helix-loop-helix-PAS heterodimer regulated by cellular O₂ tension. *Proc Natl Acad Sci U S A*. 1995; 92:5510–5514. [PubMed: 7539918]
5. Semenza GL. Regulation of oxygen homeostasis by hypoxia-inducible factor 1. *Physiology (Bethesda)*. 2009; 24:97–106. [PubMed: 19364912]
6. Semenza GL. Involvement of oxygen-sensing pathways in physiologic and pathologic erythropoiesis. *Blood*. 2009; 114:2015–2019. [PubMed: 19494350]
7. Tian H, McKnight SL, Russell DW. Endothelial PAS domain protein 1 (EPAS1), a transcription factor selectively expressed in endothelial cells. *Genes Dev*. 1997; 11:72–82. [PubMed: 9000051]
8. Ema M, et al. A novel bHLH-PAS factor with close sequence similarity to hypoxia-inducible factor 1 α regulates VEGF expression and is potentially involved in lung and vascular development. *Proc Natl Acad Sci USA*. 1997; 94:4273–4278. [PubMed: 9113979]
9. Flamme I, et al. HRF, a putative basic helix-loop-helix-PAS-domain transcription factor is closely related to hypoxia-inducible factor 1 α and developmentally expressed in blood vessels. *Mech Dev*. 1997; 63:51–60. [PubMed: 9178256]
10. Dioum EM, et al. Regulation of hypoxia-inducible factor 2 α signaling by the stress-responsive deacetylase sirtuin 1. *Science*. 2009; 324:1289–1293. [PubMed: 19498162]
11. Scortegagna M, et al. HIF-2 α regulates murine hematopoietic development in an erythropoietin-dependent manner. *Blood*. 2005; 105:3133–3140. [PubMed: 15626745]
12. Scortegagna M, Morris MA, Oktay Y, Bennett M, Garcia JA. The HIF family member EPAS1/HIF-2 α is required for normal hematopoiesis in mice. *Blood*. 2003; 102:1634–1640. [PubMed: 12750163]
13. Rankin EB, et al. Hypoxia-inducible factor-2 (HIF-2) regulates hepatic erythropoietin in vivo. *J Clin Invest*. 2007; 117:1068–1077. [PubMed: 17404621]
14. Warnecke C, et al. Differentiating the functional role of hypoxia-inducible factor (HIF)-1 α and HIF-2 α (EPAS-1) by the use of RNA interference: erythropoietin is a HIF-2 α target gene in Hep3B and Kelly cells. *Faseb J*. 2004; 18:1462–1464. [PubMed: 15240563]

15. Kapitsinou PP, et al. Hepatic HIF-2 regulates erythropoietic responses to hypoxia in renal anemia. *Blood*. 2010; 116:3039–3048. [PubMed: 20628150]
16. Chen R, et al. The acetylase/deacetylase couple CREB-binding protein/Sirtuin 1 controls hypoxia-inducible factor 2 signaling. *J Biol Chem*. 2012; 287:30800–30811. [PubMed: 22807441]
17. Papandreou I, Cairns RA, Fontana L, Lim AL, Denko NC. HIF-1 mediates adaptation to hypoxia by actively downregulating mitochondrial oxygen consumption. *Cell Metab*. 2006; 3:187–197. [PubMed: 16517406]
18. Kim JW, Tchernyshyov I, Semenza GL, Dang CV. HIF-1-mediated expression of pyruvate dehydrogenase kinase: a metabolic switch required for cellular adaptation to hypoxia. *Cell Metab*. 2006; 3:177–185. [PubMed: 16517405]
19. Zaidi N, Swinnen JV, Smans K. ATP-citrate lyase: a key player in cancer metabolism. *Cancer Res*. 2012; 72:3709–3714. [PubMed: 22787121]
20. Fujino T, Kondo J, Ishikawa M, Morikawa K, Yamamoto TT. Acetyl-CoA synthetase 2, a mitochondrial matrix enzyme involved in the oxidation of acetate. *J Biol Chem*. 2001; 276:11420–11426. [PubMed: 11150295]
21. Luong A, Hannah VC, Brown MS, Goldstein JL. Molecular characterization of human acetyl-CoA synthetase, an enzyme regulated by sterol regulatory element-binding proteins. *J Biol Chem*. 2000; 275:26458–26466. [PubMed: 10843999]
22. Loikkanen I, Haghighi S, Vainio S, Pajunen A. Expression of cytosolic acetyl-CoA synthetase gene is developmentally regulated. *Mech Dev*. 2002; 115:139–141. [PubMed: 12049778]
23. Barth C, Sladek M, Decker K. The subcellular distribution of short-chain fatty acyl-CoA synthetase activity in rat tissues. *Biochim Biophys Acta*. 1971; 248:24–33. [PubMed: 4334748]
24. Wellen KE, et al. ATP-citrate lyase links cellular metabolism to histone acetylation. *Science*. 2009; 324:1076–1080. [PubMed: 19461003]
25. Chen R, Dioum EM, Hogg RT, Gerard RD, Garcia JA. Hypoxia increases sirtuin 1 expression in a hypoxia-inducible factor-dependent manner. *J Biol Chem*. 2011; 286:13869–13878. [PubMed: 21345792]
26. Yoshii Y, et al. Cytosolic acetyl-CoA synthetase affected tumor cell survival under hypoxia: the possible function in tumor acetyl-CoA/acetate metabolism. *Cancer Sci*. 2009; 100:821–827. [PubMed: 19445015]
27. Lord BI, Murphy MJ Jr. Hematopoietic stem cell regulation. II. Chronic effects of hypoxic-hypoxia on CFU kinetics. *Blood*. 1973; 42:89–98. [PubMed: 4577713]
28. Itano HA, Hirota K, Hosokawa K. Mechanism of induction of haemolytic anaemia by phenylhydrazine. *Nature*. 1975; 256:665–667. [PubMed: 1153002]
29. Laderoute KR, et al. 5'-AMP-activated protein kinase (AMPK) is induced by low-oxygen and glucose deprivation conditions found in solid-tumor microenvironments. *Mol Cell Biol*. 2006; 26:5336–5347. [PubMed: 16809770]
30. Leelahavanichkul A, et al. Angiotensin II overcomes strain-dependent resistance of rapid CKD progression in a new remnant kidney mouse model. *Kidney Int*. 2010; 78:1136–1153. [PubMed: 20736988]
31. Brox AG, Zhang F, Guyda H, Gagnon RF. Subtherapeutic erythropoietin and insulin-like growth factor-1 correct the anemia of chronic renal failure in the mouse. *Kidney Int*. 1996; 50:937–943. [PubMed: 8872969]
32. Russell ES. Analysis of pleiotropism at the W-locus in the mouse; relationship between the effects of W and Wv substitution on hair pigmentation and on erythrocytes. *Genetics*. 1949; 34:708–723. [PubMed: 15393917]
33. Kabaya K, et al. Improvement of anemia in W/WV mice by recombinant human erythropoietin (rHuEPO) mediated through EPO receptors with lowered affinity. *Life Sci*. 1995; 57:1067–1076. [PubMed: 7658914]
34. Tonia T. Erythropoietin or darbepoetin for patients with cancer. *Cochrane Database Syst Rev*. 2012; 12:CD003407. [PubMed: 23235597]
35. Cao Y. Erythropoietin in cancer: a dilemma in risk therapy. *Trends Endocrinol Metab*. 2013; 24:190–199. [PubMed: 23218687]

36. Zhou B, et al. Erythropoietin promotes breast tumorigenesis through tumor-initiating cell self-renewal. *J Clin Invest*. 2014; 124:553–563. [PubMed: 24435044]
37. Yamashita H, Kaneyuki T, Tagawa K. Production of acetate in the liver and its utilization in peripheral tissues. *Biochim Biophys Acta*. 2001; 1532:79–87. [PubMed: 11420176]
38. O'Connor PM. Renal oxygen delivery: matching delivery to metabolic demand. *Clin Exp Pharmacol Physiol*. 2006; 33:961–967. [PubMed: 17002675]
39. Jungermann K, Kietzmann T. Oxygen: modulator of metabolic zonation and disease of the liver. *Hepatology*. 2000; 31:255–260. [PubMed: 10655244]
40. Rabkin M, Blum JJ. Quantitative analysis of intermediary metabolism in hepatocytes incubated in the presence and absence of glucagon with a substrate mixture containing glucose, ribose, fructose, alanine and acetate. *Biochem J*. 1985; 225:761–786. [PubMed: 3919712]
41. Crabtree B, Gordon MJ, Christie SL. Measurement of the rates of acetyl-CoA hydrolysis and synthesis from acetate in rat hepatocytes and the role of these fluxes in substrate cycling. *Biochem J*. 1990; 270:219–225. [PubMed: 2396982]
42. Crabtree B, Marr SA, Anderson SE, MacRae JC. Measurement of the rate of substrate cycling between acetate and acetyl-CoA in sheep muscle in vivo. Effects of infusion of acetate. *Biochem J*. 1987; 243:821–827. [PubMed: 3663102]
43. Crabtree B, Newsholme EA. Sensitivity of a near-equilibrium reaction in a metabolic pathway to changes in substrate concentration. *Eur J Biochem*. 1978; 89:19–22. [PubMed: 699906]
44. McBrien MA, et al. Histone acetylation regulates intracellular pH. *Mol Cell*. 2013; 49:310–321. [PubMed: 23201122]
45. Gordon MJ, Crabtree B. The effects of propionate and butyrate on acetate metabolism in rat hepatocytes. *Int J Biochem*. 1992; 24:1029–1031. [PubMed: 1397495]
46. Waniewski RA, Martin DL. Preferential utilization of acetate by astrocytes is attributable to transport. *J Neurosci*. 1998; 18:5225–5233. [PubMed: 9651205]
47. Mahon PC, Hirota K, Semenza GL. FIH-1: a novel protein that interacts with HIF-1 α and VHL to mediate repression of HIF-1 transcriptional activity. *Genes Dev*. 2001; 15:2675–2686. [PubMed: 11641274]
48. Lando D, et al. FIH-1 is an asparaginyl hydroxylase enzyme that regulates the transcriptional activity of hypoxia-inducible factor. *Genes Dev*. 2002; 16:1466–1471. [PubMed: 12080085]
49. Bracken CP, et al. Cell-specific regulation of hypoxia-inducible factor (HIF)-1 α and HIF-2 α stabilization and transactivation in a graded oxygen environment. *J Biol Chem*. 2006; 281:22575–22585. [PubMed: 16760477]
50. Wu DC, Paulson RF. Hypoxia regulates BMP4 expression in the murine spleen during the recovery from acute anemia. *PLoS One*. 2010; 5:e11303. [PubMed: 20585586]
51. Ball AM, Winstead PS. Recombinant human erythropoietin therapy in critically ill Jehovah's Witnesses. *Pharmacotherapy*. 2008; 28:1383–1390. [PubMed: 18956998]
52. Mansell MA, Wing AJ. Acetate or bicarbonate for haemodialysis? *Br Med J (Clin Res Ed)*. 1983; 287:308–309.
53. Suzuki M, Hirasawa Y. Correction of metabolic acidosis and changes in plasma acetate levels in acetate and bicarbonate dialyses and acetate-free biofiltration. *Contrib Nephrol*. 1994; 108:114–120. [PubMed: 8039392]
54. Veech RL, Gitomer WL. The medical and metabolic consequences of administration of sodium acetate. *Adv Enzyme Regul*. 1988; 27:313–343. [PubMed: 2854950]
55. Masuda A, et al. Effects of acetate-free citrate dialysate on glycooxidation and lipid peroxidation products in hemodialysis patients. *Nephron Extra*. 2012; 2:256–268. [PubMed: 23599704]
56. Grover A, et al. Erythropoietin guides multipotent hematopoietic progenitor cells toward an erythroid fate. *J Exp Med*. 2014; 211:181–188. [PubMed: 24493804]
57. Ariyannur PS, et al. Nuclear-cytoplasmic localization of acetyl coenzyme a synthetase-1 in the rat brain. *J Comp Neurol*. 2010; 518:2952–2977. [PubMed: 20533355]
58. Chavez JC, Baranova O, Lin J, Pichiule P. The transcriptional activator hypoxia inducible factor 2 (HIF-2/EPAS-1) regulates the oxygen-dependent expression of erythropoietin in cortical astrocytes. *J Neurosci*. 2006; 26:9471–9481. [PubMed: 16971531]

59. Scortegagna M, et al. Multiple organ pathology, metabolic abnormalities and impaired homeostasis of reactive oxygen species in *Epas1*^{-/-} mice. *Nat Genet.* 2003; 35:331–340. [PubMed: 14608355]
60. Kojima I, et al. Protective role of hypoxia-inducible factor-2alpha against ischemic damage and oxidative stress in the kidney. *J Am Soc Nephrol.* 2007; 18:1218–1226. [PubMed: 17344427]
61. Sun D, Melegari M, Sridhar S, Rogler CE, Zhu L. Multi-miRNA hairpin method that improves gene knockdown efficiency and provides linked multi-gene knockdown. *Biotechniques.* 2006; 41:59–63. [PubMed: 16869514]
62. Stegmeier F, Hu G, Rickles RJ, Hannon GJ, Elledge SJ. A lentiviral microRNA-based system for single-copy polymerase II-regulated RNA interference in mammalian cells. *Proc Natl Acad Sci U S A.* 2005; 102:13212–13217. [PubMed: 16141338]
63. Sowter HM, Raval RR, Moore JW, Ratcliffe PJ, Harris AL. Predominant role of hypoxia-inducible transcription factor (Hif)-1alpha versus Hif-2alpha in regulation of the transcriptional response to hypoxia. *Cancer Res.* 2003; 63:6130–6134. [PubMed: 14559790]
64. Aprelikova O, et al. Regulation of HIF prolyl hydroxylases by hypoxia-inducible factors. *J Cell Biochem.* 2004; 92:491–501. [PubMed: 15156561]
65. Carroll VA, Ashcroft M. Role of hypoxia-inducible factor (HIF)-1alpha versus HIF-2alpha in the regulation of HIF target genes in response to hypoxia, insulin-like growth factor-I, or loss of von Hippel-Lindau function: implications for targeting the HIF pathway. *Cancer Res.* 2006; 66:6264–6270. [PubMed: 16778202]
66. Soriano P, Montgomery C, Geske R, Bradley A. Targeted disruption of the *c-src* proto-oncogene leads to osteopetrosis in mice. *Cell.* 1991; 64:693–702. [PubMed: 1997203]
67. Shimano H, et al. Elevated levels of SREBP-2 and cholesterol synthesis in livers of mice homozygous for a targeted disruption of the SREBP-1 gene. *J Clin Invest.* 1997; 100:2115–2124. [PubMed: 9329978]
68. Cohen J. A power primer. *Psychological Bulletin.* 1992; 112:155–159. [PubMed: 19565683]
69. Denenberg VH. A Primer for Behavioral Research. *Mental Retardation and Developmental Disabilities Research Reviews.* 1996; 2:209–215.

The abbreviations used are

A, Ac	acetate
Acly	ATP citrate lyase
ACS	acetyl CoA synthetase
Acss1	acetyl CoA synthetase 1
Acss2	acetyl CoA synthetase 2
B, Bu	butyrate
CBP	Creb binding protein
Con	control
CTAD	carboxy (C)-terminal activation domain
Epo	erythropoietin
ESRD	end-stage renal disease
FIH1	Factor Inhibiting HIF-1
GTA	glyceryl triacetate
GTB	glyceryl tributyrates

GTP	glyceryl tripropionate
HIF	Hypoxia Inducible Factor
HRE	HIF-responsive element
IB	immunoblot
IP	immunoprecipitation
KO	knockout
MUT	mutant
NAM	nicotinamide
P, Pr	propionate
PDH	pyruvate dehydrogenase
PHZ	phenylhydrazine
PMSF	phenylmethylsulfonyl fluoride
SCFA	short chain fatty acids
SD	standard deviation
SEM	standard error of the mean
Sirt1	Sirtuin 1
V, Veh	vehicle
WT	wild-type

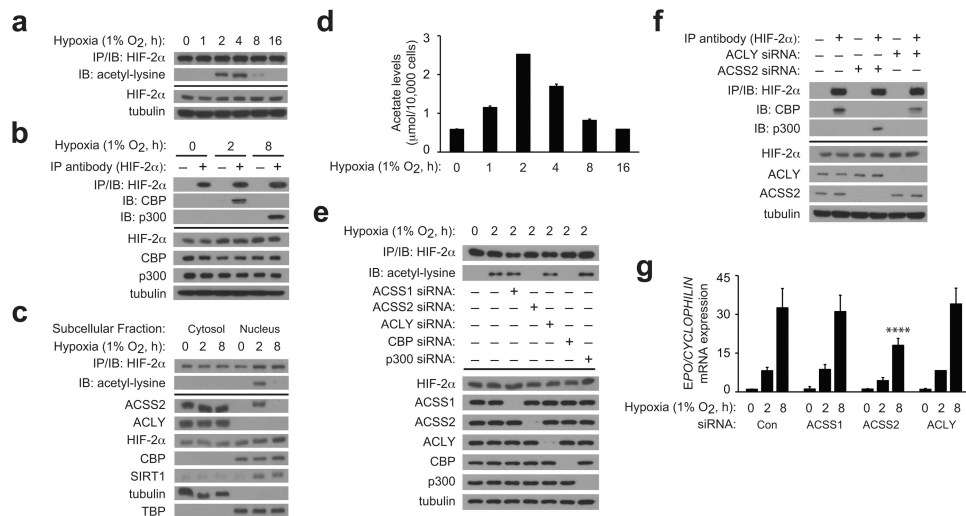


Figure 1. Acss2 controls HIF-2 signaling in hypoxic cells
(a) Time course of endogenous HIF-2α acetylation during hypoxia following immunoprecipitation (IP) of HIF-2α from whole cell extracts and detection of acetylated lysines by immunoblotting (IB). **(b)** Endogenous CBP/HIF-2α or p300/HIF-2α complex formation after hypoxia exposure. **(c)** Subcellular localization of ACSS2, ACLY, HIF-2α, CBP, and SIRT1 following hypoxia exposure. Also shown is endogenous acetylated HIF-2α present in each fraction. **(d)** Acetate levels in cells during hypoxia ($n=3$ biological replicates/time-point; single measurement/replicate; mean/SD). **(e)** Contribution of ACSS1, ACSS2, ACLY, CBP and p300 to endogenous HIF-2α acetylation during early (2 h) hypoxia. **(f)** Contribution of ACLY and ACSS2 to endogenous CBP/HIF-2α or p300/HIF-2α complex formation during early (2 h) hypoxia. **(g)** Contribution of ACSS1, ACSS2, and ACLY to *EPO* gene expression following hypoxia exposure (single pool of triplicate biological replicates/manipulation; triplicate measurements/pool; mean/SD). Separate analyses of 0, 2, and 8 h hypoxia samples was performed by two-way ANOVA with Dunnett's multiple comparison post-hoc test using control siRNA as reference within each group; only results for 8 h hypoxia are indicated (**** P 0.0001). All experiments were performed with Hep3B cells and key aspects of the above findings have been confirmed by at least one additional independent experiment.

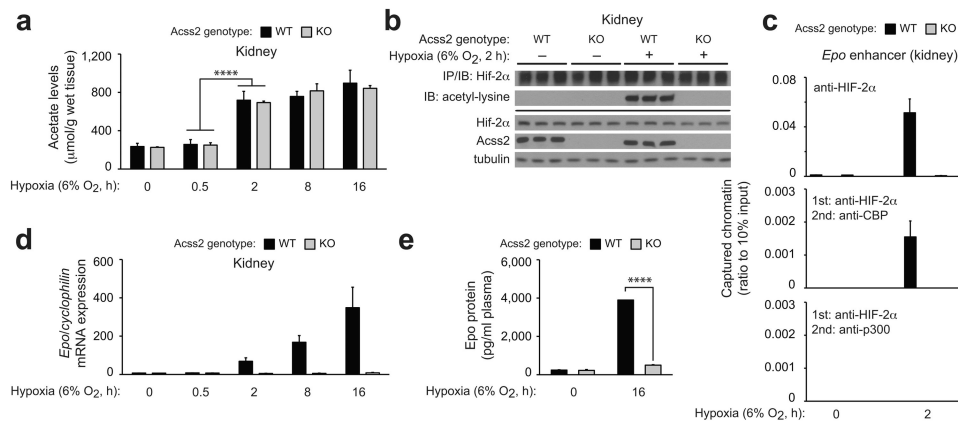


Figure 2. *Acss2* regulates hypoxia-induced renal *Epo* expression in mice

(a) Acetate levels in kidneys of *Acss2* wild-type (WT) or knockout (KO) mice exposed to normoxia or hypoxia ($n=3$ biological replicates/group, 3 male mice for 8 h time-point, 2 male and 1 female mice for other time-points; single measurements/replicate; mean/SD). Comparison of means was performed by two-way ANOVA with Dunnett's multiple comparison post-hoc test (**** P 0.0001). (b) Acetylation of endogenous HIF-2 α isolated by immunoprecipitation (IP) from kidney extracts of *Acss2* WT or KO mice and detected by immunoblotting (IB) with anti-acetylated lysine or anti-HIF-2 α antibodies. (c) Recruitment of HIF-2 α as well as coupled recruitment of HIF-2 α with CBP or p300 to the *Epo* enhancer in kidneys of mixed strain *Acss2* WT or KO mice maintained under normoxia or short-term (2 h) continuous hypoxia ($n=4$ biological replicates/group, 2 male and 2 female mice/group; duplicate measurements/replicate; mean/SEM). (d) *Epo* gene expression in kidneys of *Acss2* KO and WT mice following normoxia or hypoxia exposure ($n=3$ biological replicates/group, 3 male mice for 8 h time-point, 2 male and 1 female mice for other time-points; triplicate measurements/replicate; mean/SEM). (e) *Epo* protein measurements of plasma from *Acss2* KO and WT mice housed under normoxia or 16 h hypoxia ($n=3$ biological replicates/group; 2 male, 1 female mice/group; duplicate measurements/replicate; mean/SEM). All comparisons by unpaired Student's t-test with Holm-Sidak correction (**** P 0.0001). Key aspects of the above findings have been confirmed by at least one additional independent experiment, except for (c).

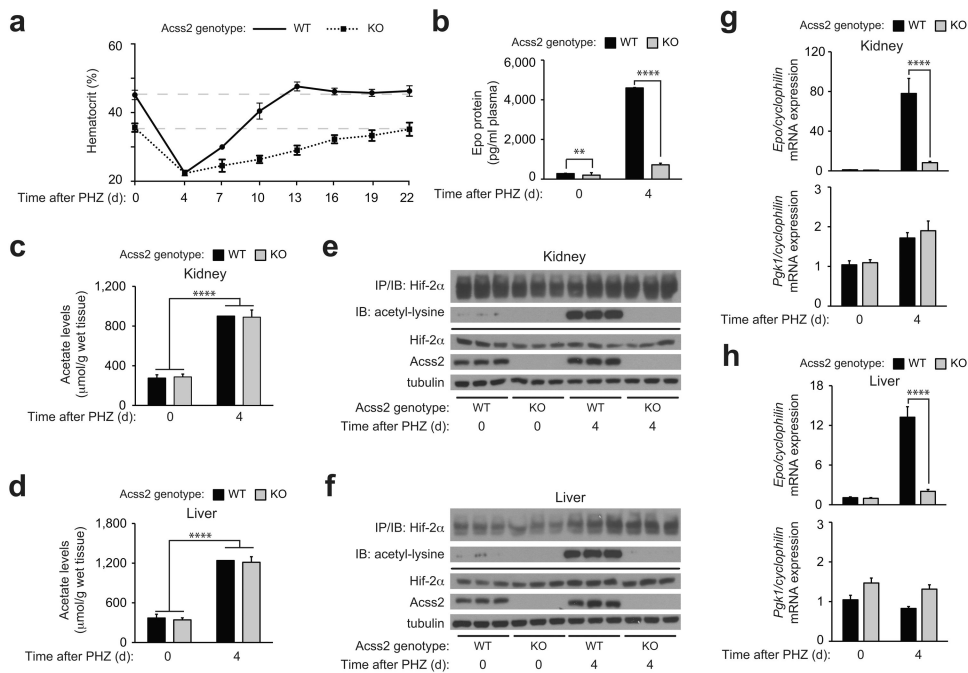


Figure 3. Acute anemia induces *Acss2*-dependent HIF-2 signaling in mice

(a) Serial hematocrits ($n=6$ biological replicates/group, 4 male and 2 female mice/group; single measurements/replicate; mean/SD) and (b) plasma Epo protein measurements ($n=8$ biological replicates/group, 8 male mice/group; duplicate measurements/replicate; mean/SEM) of mixed strain *Acss2* wild-type (WT) or knockout (KO) mice after phenylhydrazine (PHZ) treatment. Acetate levels in (c) kidneys and (d) livers of *Acss2* WT or KO mice following PHZ treatment ($n=10$ biological replicates/group, 5 male and 5 female mice/group; single measurements/replicate; mean/SD). All comparisons by unpaired Student's *t*-test with Holm-Sidak correction (** P 0.01, **** P 0.0001). Immunoblot (IB) of acetylated lysine residues following immunoprecipitation (IP) with anti-HIF-2 α antibody using (e) kidney or (f) liver extracts derived from three *Acss2* WT or KO mice chosen at random from each group in (b). *Epo* and *Pgk1* gene expression in (g) kidneys and (h) livers of same mice in (c) and (d) ($n=10$ biological replicates/group, 5 male and 5 female mice/group; duplicate measurements/replicate; mean/SEM). All comparisons by two-way ANOVA followed by Tukey's multiple comparison post-hoc test (**** P 0.0001). Key aspects of the above findings have been confirmed by at least one additional independent experiment, except for (c) and (d).

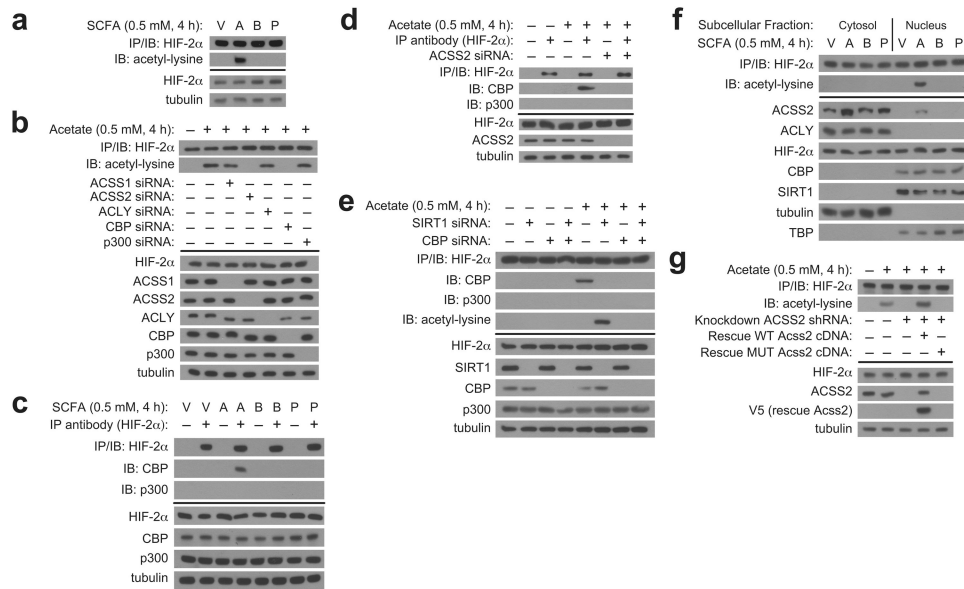


Figure 4. An acetate switch regulates Cbp/HIF-2 interactions in cells

(a) Endogenous HIF-2α acetylation following immunoprecipitation (IP) of endogenous HIF-2α and detection by immunoblotting (IB) with anti-acetylated lysine or anti-HIF-2α antibodies after incubation using medium supplemented with vehicle (V; PBS) or the short chain fatty acid (SCFA) sodium acetate (A), sodium butyrate (B), or sodium propionate (P) prepared in PBS. (b) Contribution of ACSS1, ACSS2, ACLY, CBP and p300 to endogenous HIF-2α acetylation for cells incubated using complete medium supplemented with vehicle or acetate. (c) Endogenous CBP/HIF-2α complexes formed after treatment with SCFA-containing medium. (d) Contribution of ACSS2 to endogenous CBP/HIF-2α complex formation induced by acetate treatment. (e) Endogenous CBP/HIF-2α complexes and acetylated HIF-2α induced by acetate treatment following SIRT1, CBP, or combined SIRT1/CBP knockdown. (f) Subcellular localization of ACSS2, ACLY, HIF-2α, CBP, and SIRT1 following treatment with SCFA-containing medium. (g) Endogenous HIF-2α acetylation induced by acetate supplementation in stably transformed knockdown/rescue cells expressing either an shRNA-resistant wild-type (WT) or mutant (MUT) Acss2 rescue cDNA. All experiments were performed with Hep3B cells. Key aspects of the above findings have been confirmed by at least one additional independent experiment.

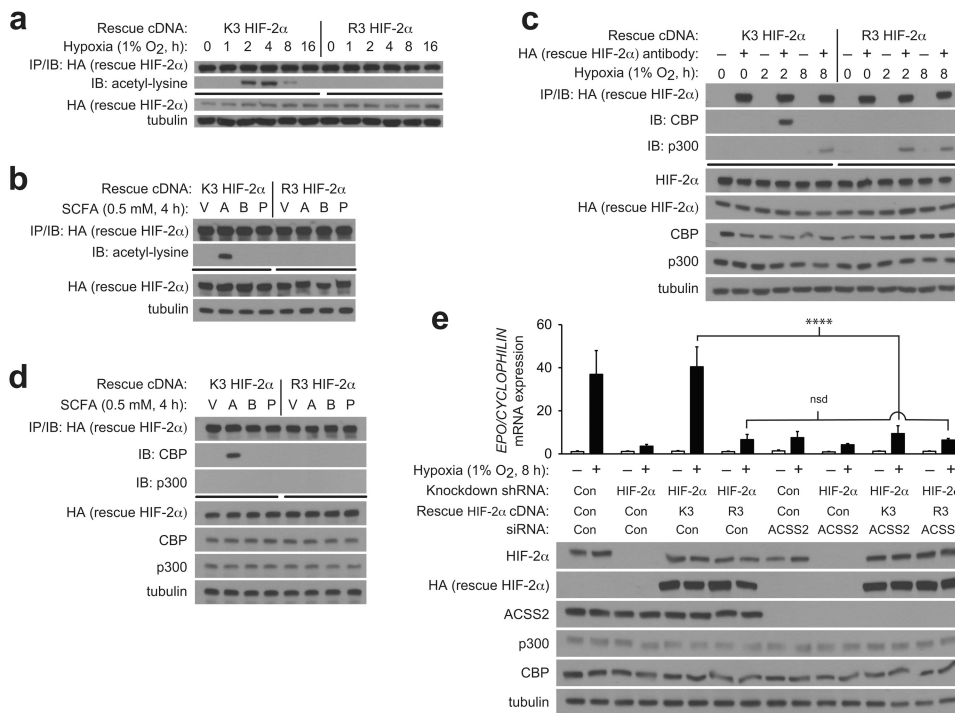


Figure 5. Acss2 signaling in cells requires intact HIF-2 acetylation

Acetylation of ectopic rescue wild-type acetylase-sensitive (K3) or acetylase-insensitive (R3) human HIF-2α after immunoprecipitation (IP) of rescue HIF-2α, followed by immunoblotting (IB) of rescue HIF-2α or acetyl-lysine after (a) hypoxia exposure or (b) supplementation of medium with PBS vehicle (V), acetate (A), butyrate (B), or propionate (P). Immunoprecipitation of ectopic rescue K3 or R3 human HIF-2α after (c) hypoxia exposure or (d) supplementation with V, A, B, or P. (e) Measurements of *EPO* gene expression in stably transformed knockdown/rescue cells expressing ectopic rescue K3 or R3 human HIF-2α and transfected with control or *Acss2* siRNA, followed by incubation under either normoxic or hypoxic conditions (single pool of triplicate biological replicates/manipulation, triplicate measurements/pool, mean/SD). All comparisons by two-way ANOVA with Tukey's multiple comparison post-hoc test (nsd, no significant difference; *****P* 0.0001). All experiments were performed with Hep3B cells. Key aspects of the above findings have been confirmed by at least one additional independent experiment.

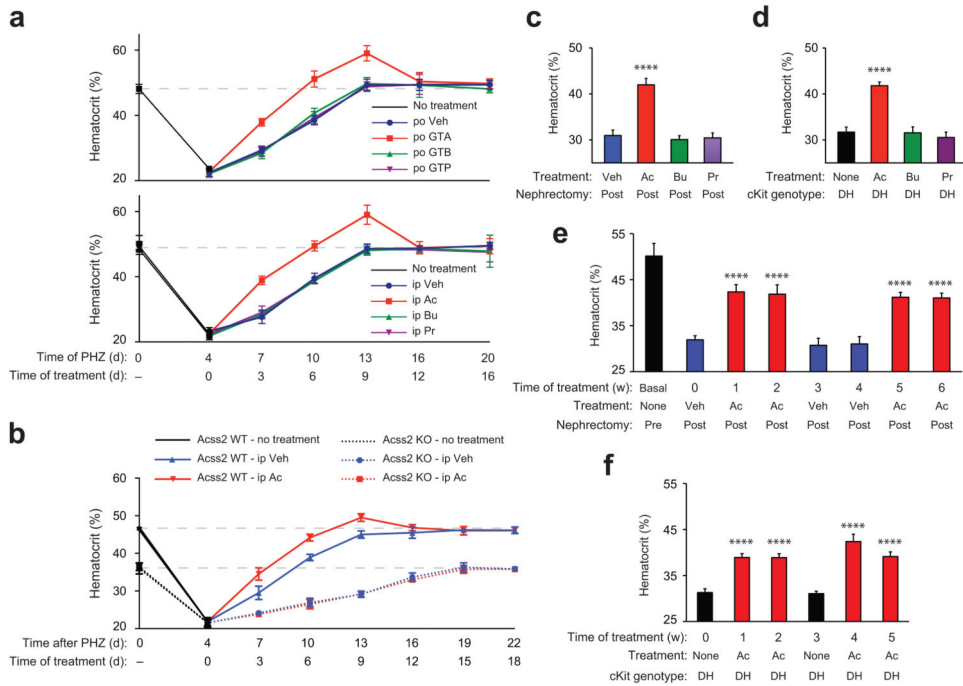


Figure 6. Acetate facilitates recovery from anemia

(a) Hematocrits of CD1 wild-type female mice after phenylhydrazine (PHZ) treatment, followed by once daily per os (po) supplementation with water vehicle (Veh; $n=7$ biological replicates), glyceryl triacetate (GTA; $n=6$ biological replicates), glyceryl tributyrate (GTB; $n=8$ biological replicates), or glyceryl tripropionate (GTP; $n=7$ biological replicates) (single measurement/replicate; mean/SD), or followed by once daily intra-peritoneal (ip) supplementation with PBS vehicle (Veh), acetate (Ac), butyrate (Bu), or propionate (Pr) ($n=5$ biological replicates/group; single measurement/replicate; mean/SD). The dotted line indicates the mean hematocrit for control CD1 wild-type female mice ($n=33$ biological replicates). (b) Serial hematocrits of mixed strain *Acss2* wild-type (WT) or knockout (KO) mice after PHZ treatment, followed by once daily ip Veh or Ac injections ($n=4$ biological replicates/group except for days 16, 19 and 22 where $n=3$ biological replicates for *Acss2* KO mice treated with Ac following death of one mouse; single measurement/replicate; mean/SD). (c) Hematocrits of CD1 wild-type female mice with chronic renal failure (CRF) induced by 5/6 partial nephrectomy and supplemented with three (Monday, M/Wednesday, W/Friday, F) ip injections of Veh ($n=11$ biological replicates), Ac ($n=11$ biological replicates), Bu ($n=8$ biological replicates), or Pr ($n=8$ biological replicates) (single measurement/replicate; mean/SD). (d) Hematocrits of WBB6 F1 hybrid double heterozygous (DH) *cKit* mutant mice with no supplements (None) or supplemented with three (M/W/F) ip injections of Ac, Bu, or Pr ($n=4$ biological replicates/group; single measurements, mean/SD). (e) Serial hematocrits of CD1 wild-type female mice before (Pre) or after (Post) partial 5/6 nephrectomy, followed by thrice-weekly (M/W/F) ip supplements of Veh or Ac ($n=8$ biological replicates/group; single measurement/replicate; mean/SD). (f) Serial hematocrits of WBB6 F1 hybrid DH *cKit* mutant mice without or with thrice-weekly (M/W/F) ip Ac supplementation ($n=4$ biological replicates/group, 2 male and 2 female mice/group; single measurement/replicate; mean/SD). Hematocrits for (c) through (f) were

obtained on the Monday following the indicated treatment period. Key aspects of the above findings have been confirmed by at least one additional independent experiment.

Author Manuscript

Author Manuscript

Author Manuscript

Author Manuscript